Ophiorrhiza Pumila Extract Exhibits Tumor-suppressive Activity in a Mouse Lymphoma Model

Lixia Fan
Foshan University
Wanqin Liao
Foshan University
Zezhen Chen
Foshan University
Shaojing Li
Foshan University
Anping Yang
Foshan University
Min-Min Chen
Foshan University
Hui Liu
Foshan University
Fang Liu (✉ 870247953@qq.com)
Foshan University

Research

Keywords: Ophiorrhiza pumila extract, lymphoma, anti-cancer activity, proliferation, EGFR

Posted Date: October 28th, 2021

DOI: https://doi.org/10.21203/rs.3.rs-965012/v1

Abstract

Background

Relapse and drug resistance of lymphomas are common, howerver the treatment efficacy of current therapeutic strategies remains unsatisfied. Our current study revealed that the extract of *Ophiorrhiza pumila* (OPE) has a potential anti-liver cancer activity. In this study, we aimed to investigate the effect of OPE on preventing lymphomas and explored the underlying mechanisms.

Methods

CCK-8 assay was applied to detect the effect of OPE on cell proliferation. Flow cytometry was used to analyzed the effect of OPE on cell cycle distribution, and apoptosis. Xenograft mouse model was conducted to determine the anti-tumor activity of OPE. TNUEL assay was performed to detect the apoptosis in tumor tissues. Western blot and immunohistochemistry were used to determined protein expression.

Results

OPE decreased A20 cell proliferation in a dose- and time-dependent manner. OPE treatment induced cell cycle arrest at S phase and elevated apoptosis in A20 cells. Moreover, OPE displayed a significant inhibition in tumor growth in a mouse model. OPE increased apoptosis in tumor tissues revealed by TUNEL assay, which was companied with enhanced cleaved caspase 3 expression and Bax/Bcl2 ratio. In addition, our data showed that OPE suppressed A20 cell viability partially by reducing EGFR phosphorylation.

Conclusions

Our data showed that OPE has an inhibitory effect on A20 cell proliferation and tumor growth, which is mediated by inactivation of EGFR and enhanced apoptosis.

Background

Lymphomas are a heterogeneous group of molecularly, biologically, and clinically distinct lymphoproliferative malignancies [1]. Multiple therapies, such as chemotherapy, radiotherapy, immunotherapy, and target therapy, have been developed for the treatment of lymphomas [2]. Although promising effects have been achieved by approaches, relapse and drug resistance are common. Therefore, developing novel strategies for lymphomas remains a primary concern currently [3]. We had previously identified that the soluble form of CXCL16 and TNF-α may be used as prognostic markers and their combinational use is a promising approach in the context of diffuse large B-cell lymphoma therapy [4].

Anti-cancer agents derived from natural plants have been reported to exhibit low toxicity and effective therapeutic activity in different types of tumors [5-7]. *Ophiorrhiza pumila* (*O. pumila*) is a Rubiaceae family plant that grows in many Asia countries, such as Japan, Vietnam, Philippines and China [8]. *O. pumila* has been considered to be a valuable alternative source of camptothecin (CPT), which is wildly used to treat various cancers, such as colorectal, ovarian, and lung cancer [9,10]. Studies refer to the biosynthesis process of CPT in *O. pumila* are decumulating [8,11,12], but the function of *O. pumila* compounds in cancer have rarely been explored. Previously, we reported that treatment with *O. pumila* extract (OPE) suppresses the proliferation and migration of liver cancer cells, indicating an anti-cancer activity of OPE in hepatocarcinoma [13]. However, the effect of compounds of *O. pumila* on other type of cancers remains unknown.

In this study, we aimed to investigate the cytotoxicity of OPE in lymphomas by using a mouse model, which may expand our understanding of the anti-cancer activity of OPE and may pay a foundation for the discovery of novel compounds against B cell lymphomas from *O. pumila*.

Methods

Reagents and materials

Antibodies against cleaved caspase-3, Bcl-2, Bax, GAPDH, and HRP-conjugated secondary antibodies were purchased from Cell Signaling Technology (Beverly, MA, USA.). Antibodies against Cylcin D1, Cyclin A2, Cyclin B1 were purchased from Proteintech (Chicago, USA). OPE was obtained as reported previously [13].

Cell culture

A20 cells were purchased from the American Type Culture Collection (ATCC, Rockville, MD, USA). A20 cells were maintained in 1640 medium plus 10% FBS and 1% penicillin/streptomycin and were incubated in an incubator with 5% CO_2 at 37°C.

Cell viability analysis

CCK-8 assay was performed to determine the viability of A20 cells after treatment with OPE. In brief, A20 cells (8~1.2 × 10^3 per well) in 100 μL completed 1640 medium were placed in 96-well plates and were exposed to different concentrations of OPE (0, 6.25, 12.5, 50, 100, and 200 μg/ml). After treatment for 24 h, 48 h, and 72 h, 10 μL of CCK-8 reagent (Dojindo, Japan) was added to each well and incubation for 2~4 h. The absorbance was then measured at 450 nm on a microplate spectrophotometer.

Cell cycle analysis

Flow cytometry was applied to investigate the influence of OPE on cell cycle distribution as described previously [13]. Briefly, A20 cells were incubated with different concentration of OPE (0, 25, 50, and 100 μg/mL). After treatment for 48 h, A20 cells were harvested, washed with PBS, and stained using the Cell

Cycle Staining Kit (MultiSciences, China). The distribution of cell cycle was analyzed by the CytoFlex-LX flow Cytometer (Beckman, USA).

Apoptosis analysis

The apoptosis of A20 cells treated with OPE was detected by using the Annexin V-FITC apoptosis detection kit (BD, USA). A20 cells (3×10^5 cells per well) were placed in 6-well plates and were exposed to different concentration of OPE (0, 25, 50 100 μg/mL). 48 h post-incubation, A20 cells were collected and washed once with PBS. A20 cells were incubated with 5 μl Annexin V-FITC and 5 μL PI in 200 μL 1×binding buffer. Then 200 μL 1×binding buffer was added to each sample. Samples were analyzed on a flow cytometer (BD Biosciences) and the data was analyzed using the CytExpert software (BD Biosciences).

Western blot analysis

A20 cells were exposed to different concentrations of OPE (0, 25, 50, and 100 μg/mL) for 48 h. A20 cells were resuspended in RIPA buffer with proteinase inhibitors (Sigma, USA) and incubated on ice for 20 min. The lysate was then centrifuged at 12,000 rpm at 4 °C for 20 min. The supernatant was collected and protein concentration was determined with the BCA protein Assay Kit (Thermo Scientific, USA). Total proteins from different samples were separated and transferred to PVDF membranes (Millipore, USA). The membrane was blocked with 5% milk in TBS-Tween for 1 h at room temperature, and was incubated with primary antibodies at 4 °C overnight. After 3 washes with TBS-Tween, the membrane was incubated with HRP-conjugated secondary antibodies at room temperature for 1 h. An enhanced chemiluminescence (ECL) kit (Millipore) was used to detect the protein bands and Image J software was used to determine the relative protein expression.

Animal experiments

Balb/c mice (6-8 weeks old) were used for the *in vivo* experiments. 5×10^6 A20 cells in PBS were subcutaneously injected into the right oxter of Balb/c mice. When the tumors reached 50~100 mm^3, mice were randomly derived into three groups: the control group, low-dose group and high-dose group (n=4). Mice in the control group were gavagely administered with PBS. Mice in the low-dose group were gavagely administrated with 15 mg/kg OPE, while mice in the high-dose group was gavagely administrated with 45 mg/kg OPE every other day. The administration was last for 10 days. Then the mice were sacrificed and tumors were isolated. The animal experiments were approved by the Institutional Animal Care and Use Committee of Foshan University.

TUNEL analysis

Tumor tissues were fixed and embedded in paraffin. Tissue sections were cut, deparaffinized, repaired with protease K, and permeabilized. Then sections were stained with the Fluorescein (FITC) TUNEL Cell

Apoptosis Detection Kit (Servicebio, Wuhan, China). The nuclei were stained with DAPI. Tumor sections were visulized under a fluorescence microscopy (Zeiss, Germany).

Immunohistochemistry

Tumor tissues were fixed with 4% paraformaldehyde and embedded into paraffin. Paraffin sections (4 μm-think) were deparaffinized, antigen-retrieved, and treated with 3% hydrogen peroxide. Then, sections were blocked with 3% BSA, followed by incubation with primary antibodies (cleaved casepase-3 and Ki-67 antibodies, Cell signaling technology) overnight at 4 °C. After washed with PBS, sections were incubated with HRP-conjugated secondary antibodies and color was detected using a DAB detection kit. Sections were counterstained with hematoxylin. Three random fields per tumor were selected and Cleaved caspase 3 and Ki-67 positive cells in each field were counted.

Statistical analysis

All experiments were repeated three times and the data were represent as means ± SD. Comparisons among more than two groups were performed by the one-way analysis of variance (ANOVA) using the SPSS 19.0 software. A $p < 0.05$ was considered statistically significant.

Results

OPE suppresses the proliferation and induces S phase arrest in A20 cells

To determine the effect of OPE on cell viability, CCk-8 assay was performed in A20 cells treated with different concentration of OPE for 24 h, 48 h, and 72 h, respectively. The results showed that treatment with OPE significantly reduce A20 cell viability, which was in a time- and dose-dependent manner (Fig.1 A-C). The IC_{50} value (50% inhibition) of OPE was 223.75 μg/mL at 24 h, 27.95 μg/mL at 48 h, and 26.4 μg/mL at 72 h.

Cell cycle arrest is an important event related to cell growth. Hence, OPE may affect the viability of A20 cells by inducing cell cycle arrest. Flow cytometry analysis showed that administration of OPE highly altered the cell cycle distribution. The percentages of A20 cells at S phase for 0 μg/mL, 25 μg/mL, 50 μg/mL, and 100 μg/mL groups were 29.7%, 37.3%, 59.5%, and 67.5%, respectively (Fig. 1D and E). In consistent with these results, Western blot analysis showed that the expression of Cyclin A2, a key mediator of S phase program was markedly reduced (Fig. 1F). Together, these results suggest that OPE could induce S phase cell cycle arrest in A20 cells.

OPE triggers apoptosis of A20 cells

Apoptosis is a key process regulated cell death. Therefore, we determine whether OPE had an impact on A20 cell apoptosis. A20 cells were treated with different concentrations of OPE, and the apoptotic rate was ascertained by flow cytometry. Exposure to OPE led to a remarkable increase in apoptotic cell population, which was in a dose-dependent manner (Fig. 2A and B). The percentages of apoptotic cells in

0 μg/mL, 25 μg/mL, 50 μg/mL, and 100 μg/mL groups were 0.38%, 13.27%, 22.28%, and 38.95%, respectively. In agreement with these results, OPE treatment significantly elevated the expressions of apoptosis proteins, Bax and cleaved-caspase 3, but had no significant effect on Bcl2 expression (Fig. 2C). The expression ration of Bax/Bcl2 was detected after OPE exposure (Fig. 2D). Together, these results indicate that OPE inhibit A20 cell growth via triggering apoptosis.

OPE represses A20 cell growth *in vivo*

Next, we determine whether OPE had an anti-lymphoma activity *in vivo* by using a xenograft mouse model. Treatment with OPE significantly decreased the tumor development of derivate from A20 cells, which was in a time- and dose-dependent manner (Fig. 3). The inhibitory rates at Day 21 for 15 mg/kg and 45 mg/kg were 58.4% and 77.9%, respectively (Fig. 3A). There was no significant difference in the body weight among different groups (Fig. 3B).

OPE induces apoptosis in A20-derived tumors

To access the effect of OPE on the apoptosis in A20-derived xenografts, TUNEL staining was performed. Consistent with in vitro results, increased TUNEL-positive cells were observed in OPE-treated groups (15 mg/kg and 45 mg/kg) compared with the NC group (Fig. 4A). Western blot analysis of the tumor tissue samples also showed that the expression levels of cleaved caspase 3 and Bax were dose-dependently increased following the treatment of OPE, while no significance in the expression of Bcl2 was observed (Fig. 4B). Consistently, treatment with OPE resulted in an increase in the expression ratio of Bax/Bcl2 in tumor tissues (Fig. 4C). In agreement with these results, immunohistochemistry staining showed that there were more cleaved caspase3-positive cells and fewer Ki67-postive cells in OPE-treated groups than in the NC group (Fig. 4D). Together, these results suggested that OPE induces A20 cell apoptosis in vivo.

OPE suppresses A20 cell proliferation via inactivation of EGFR

EGFR signaling plays a vital role in the regulation of apoptosis. Therefore, we investigated whether OPE had an effect on the activation of EGFR. Indeed, Western blot analysis showed that administration of OPE remarkable reduced the phosphorylation of EGFR in A20 cells (Fig. 5A). Similarly, the levels of p-EGFR in tumors isolated from mice treated with OPE (15 mg/kg and 45 mg/kg) was significantly decreased (Fig. 5B). Treatment with EGF could partially restore the cell viability of A20 cells (Fig. 5C). Moreover, administration of EGF restrained the enhanced effect of OPE on the apoptosis rate of A20 cells (Fig. 5D). Together, these results implied that EGFR suppression partially accounted for the anti-proliferative activity of OPE in A20 cells.

Discussion

Exploring the functional activity of the extract of a certain plant is an important step for discovering novel anti-cancer agents. In addition to alkaloids, *O. pumila* also produce anthraquinones, glucosides, and chlorogenic acid, which are potential chemoprotective compounds against cancers [10,14,15]. Although

we reported that OPE has an anti-liver cancer activity [13], but its activity in lymphoma remains unclear. In the present study, we found that OPE inhibits the proliferation and induces cell cycle arrest and apoptosis in A20 cells. Moreover, OPE suppresses A20 tumor growth in vivo. Thus, our findings highlight an anti-lymphoma of OPE.

Anti-cancer compounds commonly trigger tumor cell death via inducing cell cycle arrest [16-18]. For example, ethanolic extract of Cordyceps cicadae exerts its antitumor activity in gastric cancer cells by inducing S phase arrest [19]. Withaferin A suppresses glioblastoma cell growth in triggers G2/M arrest [20]. In our study, OPE induced S phase arrest in A20 cells. Of note, we previously reported that OPE could induced a G2/M arrest in liver cancer cells [13]. Thus, these results indicate that the action of OPE on cell cycle distribution is cell type-dependent.

Given the critical role of apoptosis in cancer cell survival [21], we also accessed the effect of OPE on apoptosis. As expected, a significant increased number of apoptotic cells was visualized in OPE-treated group compared with the control group. Consistent with the in vitro result, TUNEL assay also showed a higher apoptotic rate in A20 tumor tissues isolated form OPE-treated mice compared with those from the control mice. Furthermore, Western blot analysis showed that the expression of apoptosis-related proteins, cleaved caspase 3 and Bax, two key mediators in apoptosis process [22,23], were significantly elevated, confirming the enhanced effect of OPE on A20 cell apoptosis.

EGFR is a member of ErbB family which plays vital roles in many processes associated with tumor development, such as proliferation, survival, migration and apoptosis [24,25]. Thus, targeting EGFR signaling is considered to be a crucial strategy of cancer therapy [26]. Recent evidence has revealed that EGFR signaling is implicated in the progression of lymphoma. It has been reported that EGFR activation contributed to PDGFD induced-ibrutinib resistance in diffuse large B-cell lymphoma (DLBCL) [27]. LncRNA TUC338 promotes the proliferation of DLBCL cells via activating EGFR pathway [28]. These studies indicate that activation of EGFR signaling confers the malignance of DLBCL. Our data showed that OPE could significantly reduce the phosphorylation of EGFR. The suppression of EGFR signaling could induce apoptosis and lead to cell death, consistent with previous studies [29,30]. Moreover, restoration of EGFR activity partially reversed the effects of OPE on cell viability and apoptosis. Hence, our results indicate that EGFR suppression contributes to the anti-proliferative effect of OPE in A20 cells.

Conclusion

In conclusion, OPE mediated A20 cell growth suppression by inducing cell cycle arrest. In addition, OPE displayed a significant inhibition in tumor growth in a mouse model, which might be related to enhanced cleaved caspase 3 expression and Bax/Bcl2 ratio. Moreover, OPE exerts the proliferation-suppressive activity in A20 cells via inactivation of EGFR. Our findings imply that OPE might be a promising target for lymphoma therapy. However, the extract molecular mechanisms of the anti-lymphoma activity of OPE are still needed further investigations.

Abbreviations

OPE: ethanol extract of *O. pumila*; CCK-8: cell counting kit-8; Bcl-2: B cell lymphoma/lewkmia-*2*; Bax: BCL2-associated X protein; CPT: camptothecin; GAPDH: glyceraldehyde-3-phosphate dehydrogenase; EGFR: epidermal growth factor receptor.

Declarations

Acknowledgements

Not applicable.

Author contributions

LF and WL performed the experiments and wrote the manuscript. ZC and SL provided technology assistance. FL and HL conceived the project and designed the experiments. AY and MMC provide assistance for the revision of the manuscript. All authors read and approved the final manuscript.

Funding

This work was financially supported by the National Key Research and Development Program (No. 2018YFA0902702), the National Natural Science Foundation of China (No. 81801558), and the Guangdong Basic and Applied Basic Research Fund Project (No. 2020A1515110058 and 2019A1515110696).

Availability of data and materials

The datasets used or analyzed during the current study are available from the corresponding author on reasonable request.

Ethics approval and consent to participate

The experiment was approved by the Ethical Review Committee of the Experimental Animal Welfare, Foshan University.

Consent for publication

All of the authors were concerned and agreed to publish before the submission.

Competing interests

All authors declared no competing interests.

Author details

Department of Basic Medicine and Biomedical Engineering, School of Medicine, Foshan University, No.5, Hebin Road, Chancheng District, Foshan 528000, China.

References

1. Pasqualucci L. Molecular pathogenesis of germinal center-derived B cell lymphomas. Immunol Rev. 2019; 288:240-261.

2. Chung C. Current targeted therapies in lymphomas. Am J Health Syst Pharm. 2019; 76:1825-1834.

3. Thamm DH. Novel Treatments for Lymphoma. Vet Clin North Am Small Anim Pract. 2019; 49:903-915.

4. Yang H,Qiu B,Chen S, Xun Y,Pan Y, Chen M, Li W, Liao W, Saeed E,Yang A, Liu F. Soluble CXCL16 promotes TNF-α-induced apoptosis in DLBCL via the AMAD10-NF-κB regulatory feedback loop. Cell Biol Int. 2019; 43:863-874.

5. Efferth T, Saeed MEM, Kadioglu O, Seo EJ, Shirooie S, Mbaveng AT, Nabavi SM, Kuete V. Collateral sensitivity of natural products in drug-resistant cancer cells. Biotechnol Adv. 2020; 38:107342.

6. Agarwal G, Carcache PJB, Addo EM, Kinghorn AD. Current status and contemporary approaches to the discovery of antitumor agents from higher plants. Biotechnol Adv. 2020; 38:107337.

7. Subramaniam S, Selvaduray KR, Radhakrishnan AK. Bioactive Compounds: Natural Defense Against Cancer.Biomolecules. 2019; 9.

8. Lee JY, Hiyama M, Hikosaka S, Goto E. Effects of Concentration and Temperature of Nutrient Solution on Growth and Camptothecin Accumulation of Ophiorrhiza pumila. Plants (Basel). 2020; 9.

9. Sirikantaramas S, Sudo H, Asano T, Yamazaki M, Saito K. Transport of camptothecin in hairy roots of Ophiorrhiza pumila. Phytochemistry. 2007; 68:2881-2886.

10. Godbole RC, Pable AA, Barvkar VT. Transcriptome-wide identification, characterization, and phylogenomic analysis of cytochrome P450s from Nothapodytes nimmoniana reveal candidate genes involved in the camptothecin biosynthetic pathway. Genome. 2021; 64:1-14.

11. Wang C, Wu C, Wang Y, Xie C, Shi M, Nile S, Zhou Z, Kai G. Transcription Factor OpWRKY3 Is Involved in the Development and Biosynthesis of Camptothecin and Its Precursors in Ophiorrhiza pumila Hairy Roots. Int J Mol Sci. 2019; 20.

12. You D, Feng Y, Wang C, Sun C, Wang Y, Zhao D, Kai G. Cloning, characterization, and enzymatic identification of a new tryptophan decarboxylase from Ophiorrhiza pumila. Biotechnol Appl Biochem. 2020.

13. Liu H, Liao W, Fan L, Zheng Z, Liu D, Zhang QW, Yang A, Liu F. Ethanol extract of Ophiorrhiza pumila suppresses liver cancer cell proliferation and migration. Chin Med. 2020; 15:11.

14. Mijatovic S, Bramanti A, Nicoletti F, Fagone P, Kaluderovic GN, Maksimovic-Ivanic D. Naturally occurring compounds in differentiation based therapy of cancer. Biotechnol Adv. 2018; 36:1622-1632.

15. Wu W, Tang Y, Yang J, Idehen E, Sang S. Avenanthramide Aglycones and Glucosides in Oat Bran: Chemical Profile, Levels in Commercial Oat Products, and Cytotoxicity to Human Colon Cancer Cells. J Agric Food Chem. 2018; 66:8005-8014.

16. Suryavanshi S, Choudhari A, Raina P, Kaul-Ghanekar R. A polyherbal formulation, HC9 regulated cell growth and expression of cell cycle and chromatin modulatory proteins in breast cancer cell lines. J Ethnopharmacol. 2019; 242:112022.

17. Zhou S, Luo Q, Tan X, Huang W, Feng X, Zhang T, Chen W, Yang C, Li Y. Erchen decoction plus huiyanzhuyu decoction inhibits the cell cycle, migration and invasion and induces the apoptosis of laryngeal squamous cell carcinoma cells. J Ethnopharmacol. 2020; 256:112638.

18. Hnit SST, Yao M, Xie C, Ge G, Bi L, Jin S, Jiao L, Xu L, Long L, Nie H, Jin Y, Rogers L, Suchowerska N, Wong M, Liu T, De Souza P, Li Z, Dong Q. Transcriptional regulation of G2/M regulatory proteins and perturbation of G2/M Cell cycle transition by a traditional Chinese medicine recipe. J Ethnopharmacol. 2020; 251:112526.

19. Xie H, Li X, Chen Y, Lang M, Shen Z, Shi L. Ethanolic extract of Cordyceps cicadae exerts antitumor effect on human gastric cancer SGC-7901 cells by inducing apoptosis, cell cycle arrest and endoplasmic reticulum stress. J Ethnopharmacol. 2019; 231:230-240.

20. Tang Q, Ren L, Liu J, Li W, Zheng X, Wang J, Du G. Withaferin A triggers G2/M arrest and intrinsic apoptosis in glioblastoma cells via ATF4-ATF3-CHOP axis. Cell Prolif. 2020; 53:e12706.

21. Portt L, Norman G, Clapp C, Greenwood M, Greenwood MT. Anti-apoptosis and cell survival: a review. Biochim Biophys Acta. 2011; 1813:238-259.

22. Gu YY, Chen MH, May BH, Liao XZ, Liu JH, Tao LT, Man-Yuen Sze D, Zhang AL, Mo SL. Matrine induces apoptosis in multiple colorectal cancer cell lines in vitro and inhibits tumour growth with minimum side effects in vivo via Bcl-2 and caspase-3. Phytomedicine. 2018; 51:214-225.

23. Zhang G, Zeng X, Zhang R, Liu J, Zhang W, Zhao Y, Zhang X, Wu Z, Tan Y, Wu Y, Du B. Dioscin suppresses hepatocellular carcinoma tumor growth by inducing apoptosis and regulation of TP53, BAX, BCL2 and cleaved CASP3. Phytomedicine. 2016; 23:1329-1336.

24. Mizukami T, Izawa N, Nakajima TE, Sunakawa Y. Targeting EGFR and RAS/RAF Signaling in the Treatment of Metastatic Colorectal Cancer: From Current Treatment Strategies to Future Perspectives. Drugs. 2019; 79:633-645.

25. Wang Z. ErbB Receptors and Cancer. Methods Mol Biol. 2017; 1652:3-35.

26. Singh D, Attri BK, Gill RK, Bariwal J. Review on EGFR Inhibitors: Critical Updates. Mini Rev Med Chem. 2016; 16:1134-1166.

27. Jin J, Wang L, Tao Z, Zhang J, Lv F, Cao J, Hu X. PDGFD induces ibrutinib resistance of diffuse large Bcell lymphoma through activation of EGFR. Mol Med Rep. 2020; 21:2209-2219.

28. Li Y, Jia Z, Zhao H, Liu X, Luo J, Cui G, Kong X. TUC338 Promotes Diffuse Large B Cell Lymphoma Growth via Regulating EGFR/PI3K/AKT Signaling Pathway. J Oncol. 2021; 2021:5593720.

29. Park HJ, Min TR, Chi GY, Choi YH, Park SH. Induction of apoptosis by morusin in human non-small cell lung cancer cells by suppression of EGFR/STAT3 activation. Biochem Biophys Res Commun. 2018; 505:194-200.

30. Min TR, Park HJ, Ha KT, Chi GY, Choi YH, Park SH. Suppression of EGFR/STAT3 activity by lupeol contributes to the induction of the apoptosis of human nonsmall cell lung cancer cells. Int J Oncol. 2019; 55:320-330.

Figures

Figure 1

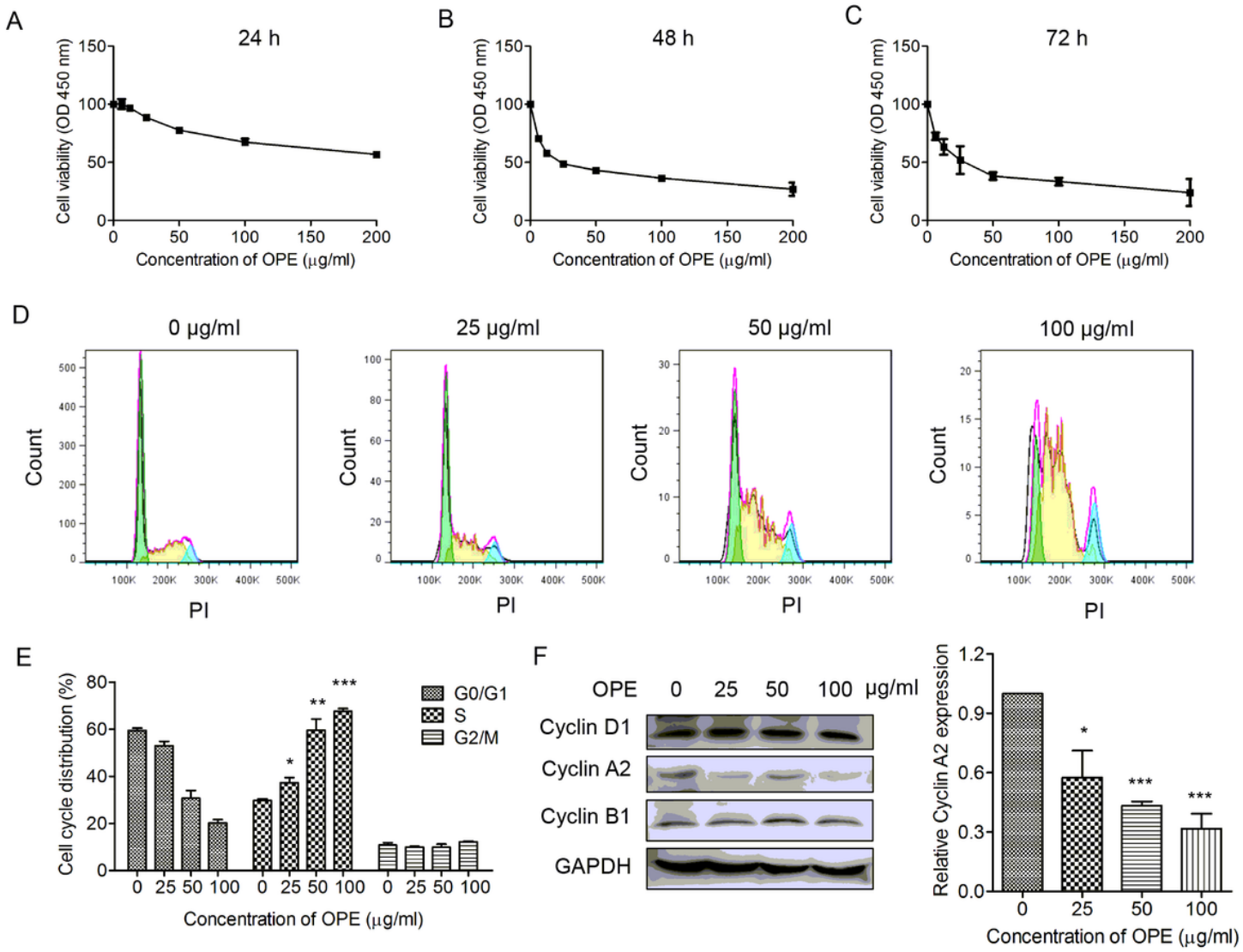

Figure 1

OPE inhibits the proliferation and induces S phase arrest in A20 cells. (A-C) OPE inhibits the proliferation of A20 cells. A20 cells were treated with different concentrations of OPE (0, 6.25, 12.5, 25, 50, and 100 μg/mL) for 24 h (A), 48 h (B), and 72 h (C), respectively, and cell viability was examined by CCK-8 assay. (D, E) OPE induces arrest in A20 cells. A20 cells were treated with different concentrations of OPE (0, 25, 50, and 100 μg/mL) for 48 h, and cell cycle distribution was accessed by flow cytometry. Data are presented as means ± SD of at least three independent experiments. (*p < 0.05; **p < 0.01;***p < 0.001, compared to the untreated control).

Figure 2

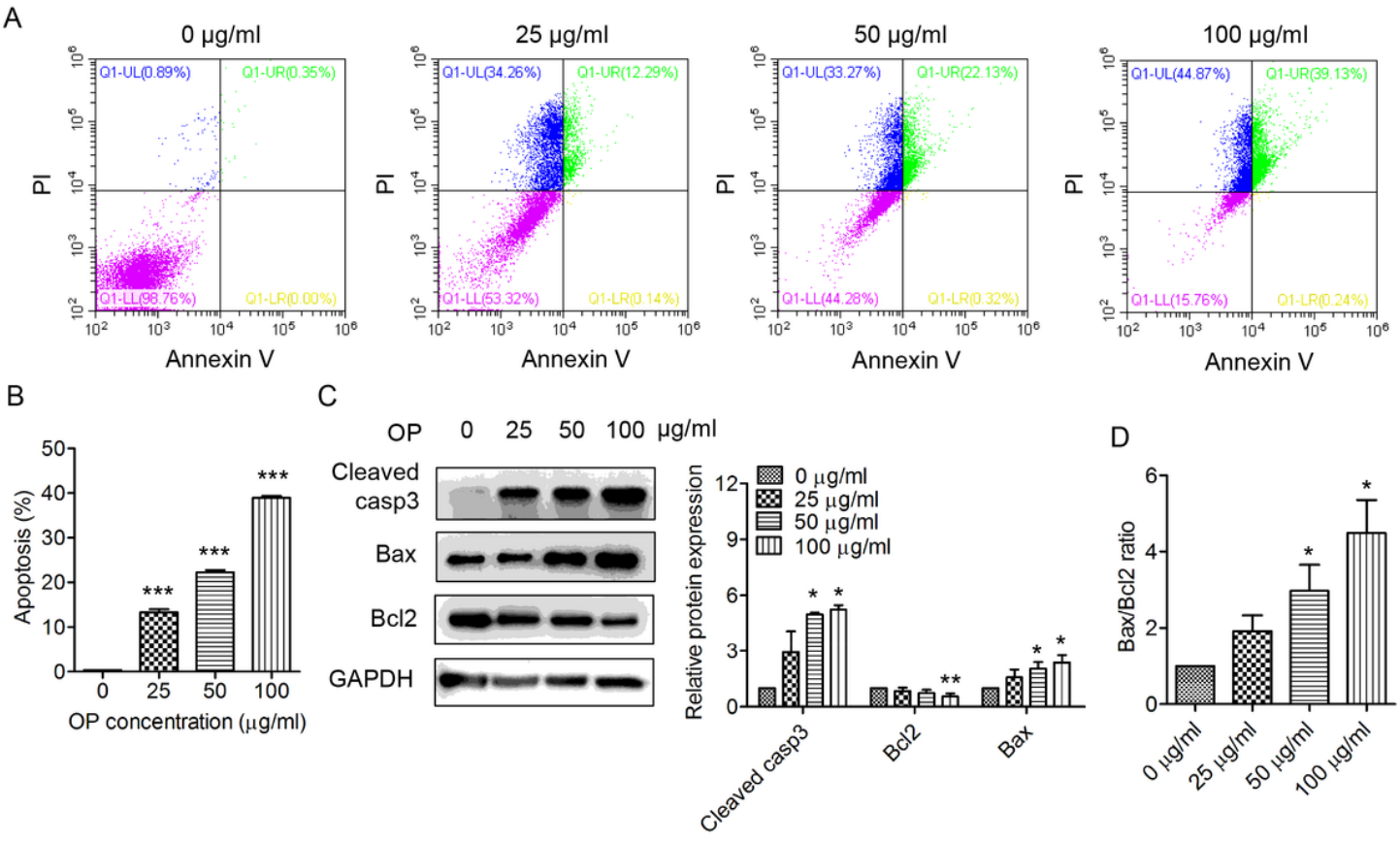

Figure 2

OPE enhances apoptosis in A20 cells. (A, B) Flow cytometry analysis of apoptosis of A20 cells after treatment with OPE (0, 25, 50, 100 μg/mL) for 48 h. (C) Western blot analysis of the expression levels of apoptosis-related proteins. A20 cells were treated with OPE (0, 6.25, 12.5, 25, 50, and 100 μg/mL) for 48 h, and Western blot was conducted with the indicated antibodies. (D) The alteration of the Bax/Bcl2 ratio in A20 cells following treatment with OPE. Data are presented as means ± SD of at least three independent experiments. (*p < 0.05; ***p < 0.001, compared to the untreated control).

Figure 3

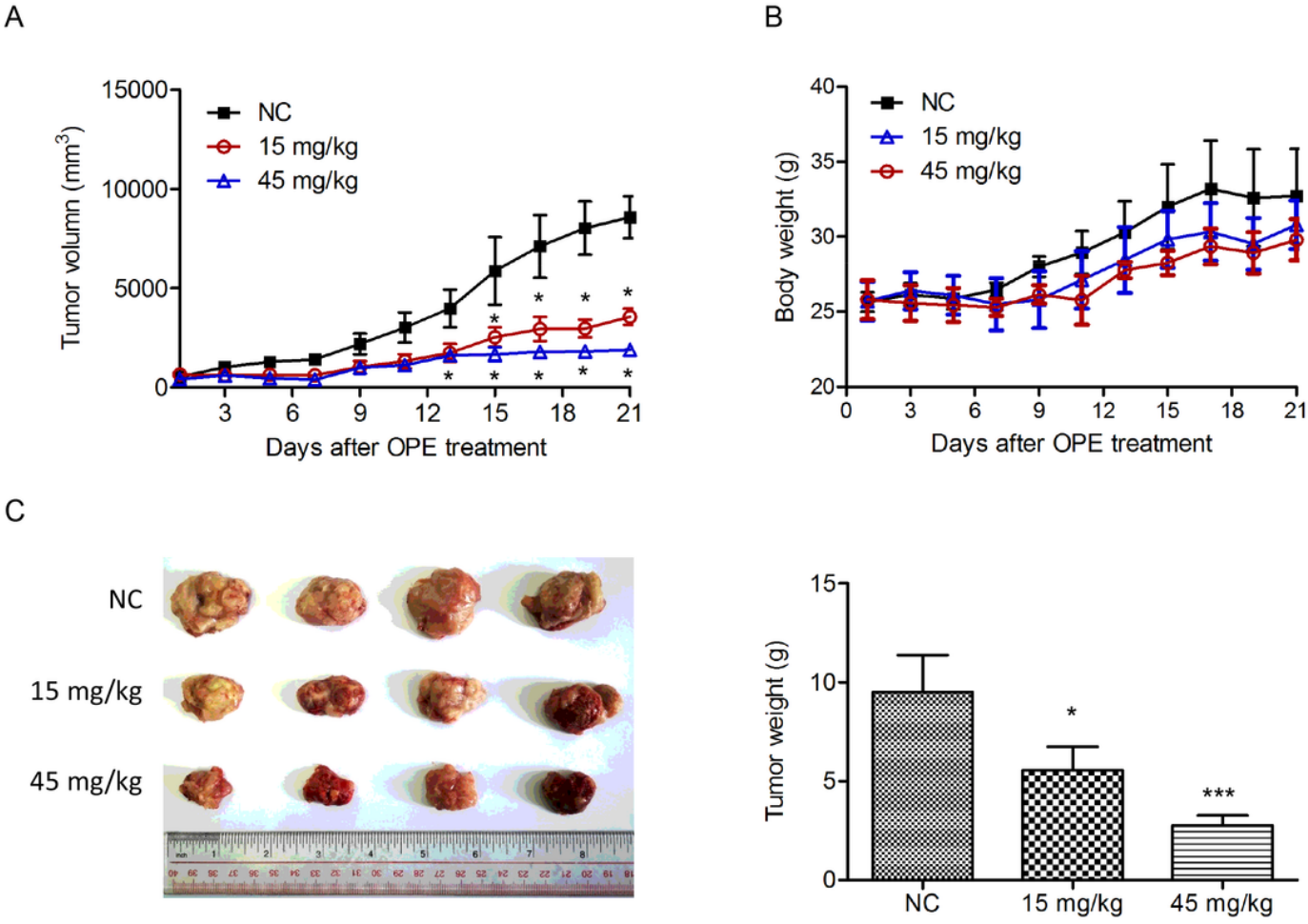

Figure 3

OPE suppresses A20 cell growth in vivo. (A) The effect of OPE on the volume of tumor derived by A20 cells. A20 cells were subcutaneously injected into the right oxter of Balb/c mice followed by the treatment with DMSO (NC), 15 mg/kg, or 45 mg/kg OPE (n=4). The tumor volume was measured every other day. (B) The body weight of Balb/c mice after tumor cell inoculation and treatment. (C) The representative images of isolated tumors from Balb/c mice. Data are presented as means ± SD. (*$p < 0.05$; ***$p < 0.001$, compared to the untreated control).

Figure 4

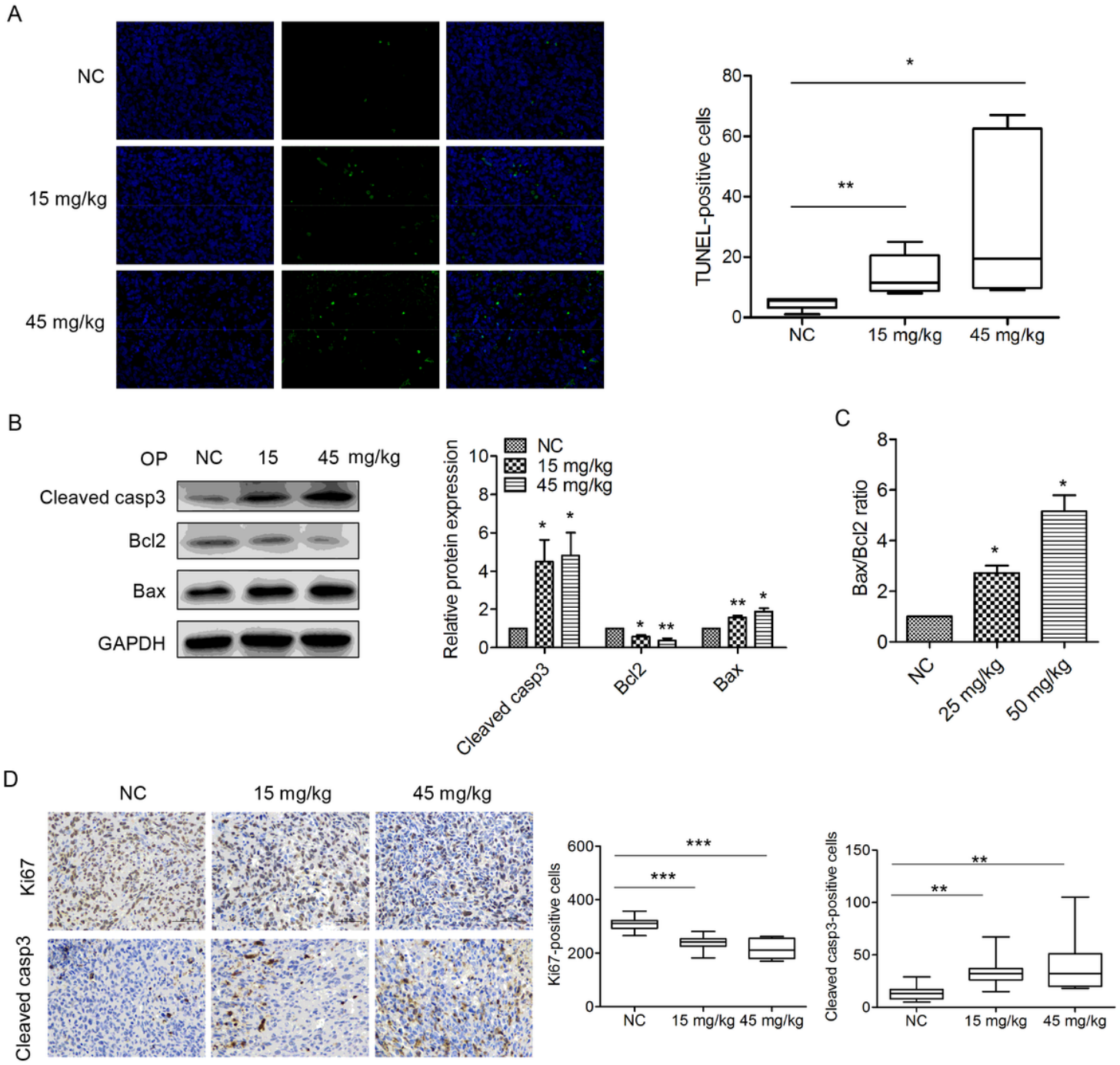

Figure 4

OPE induces apoptosis in A20-derived tumors. (A) The effect of OPE on tumor apoptosis. The tumor apoptosis was evaluated by TUNEL staining (green). DAPI (blue) was used to stained nuclei. (B) Western blot analysis of apoptosis-related proteins in tumor tissues. (C) The alteration of the Bax/Bcl2 ratio in tumor tissues following treatment with OPE. (D) Immunohistochemistry staining analysis of the cleaved caspase3-positive cells and Ki67-postive cells in tumor tissues. Data are presented as means ± SD of at

least three independent experiments. (*p < 0.05; **p < 0.01; ***p < 0.001, compared to the untreated control).

Figure 5

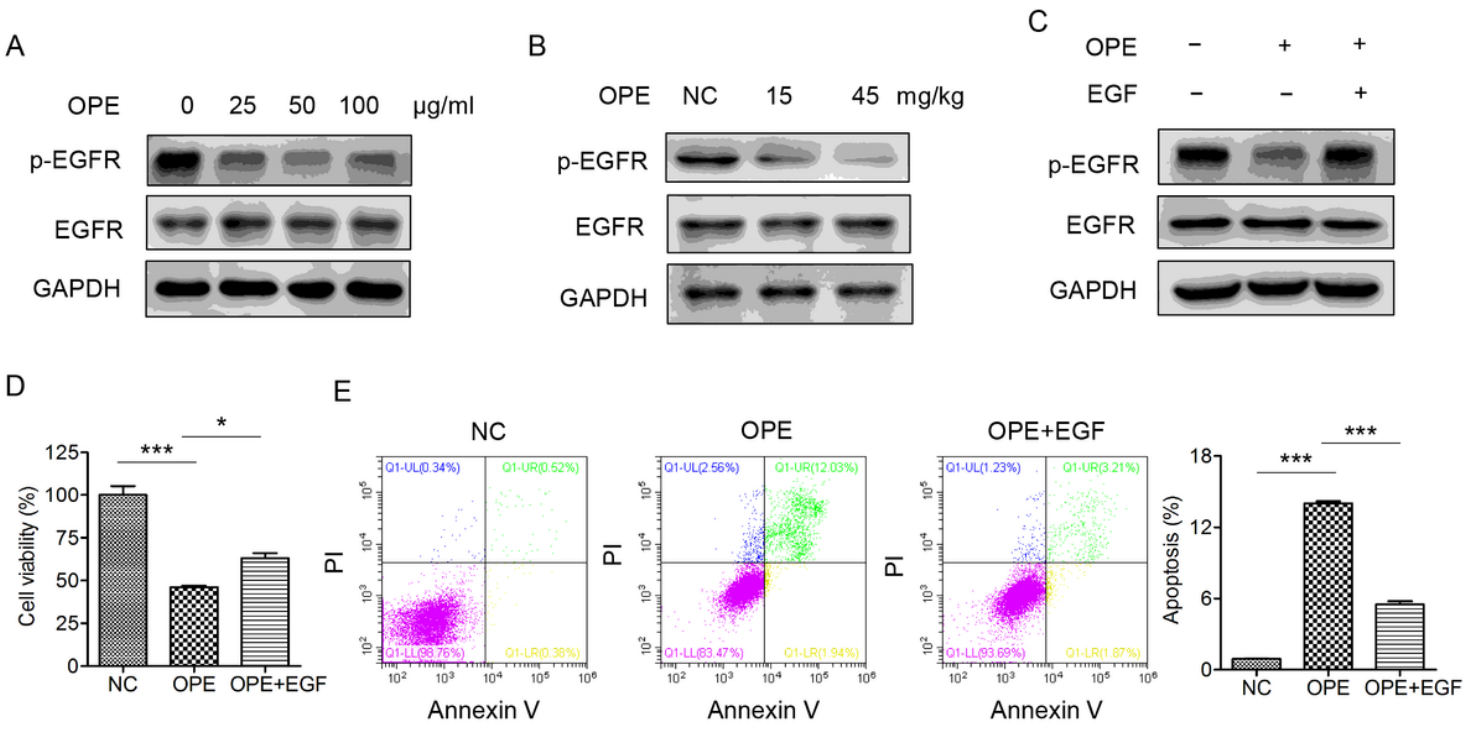

Figure 5

OPE suppresses A20 cell proliferation via inactivation of EGFR. (A) Western blot analysis of the expression and phosphorylation of EGFR in A20 cells. (B) Western blot analysis of the expression and phosphorylation of EGFR in A20 cell-derived tumors. (C) The viability of A20 cells after treatment with OPE (μg/mL) together with or without EGF (50 ng/mL). (D) The apoptosis of A20 cells after treatment with OPE (μg/mL) together with or without EGF (50 ng/mL). (E) Flow cytometry analysis of apoptosis of A20 cells treatment with OPE (μg/mL) together with or without EGF (50 ng/mL) for 48 h. Data are presented as means ± SD of at least three independent experiments. (*p < 0.05; ***p < 0.001, compared to the untreated control).